jmr&t

Journal of Materials Research and Technology

www.jmrt.com.br

abm

Original article

Characterization of nitrocarburized surface layer on AISI 1020 steel by electrolytic plasma processing in an urea electrolyte

Mehdi Karimi Zarchi[a,], Mohamad Hosein Shariat[a], Seyed Abolghasem Dehghan[a], Soheil Solhjoo[a,b]*

[a] *Department of Materials Science and Engineering, School of Engineering, Shiraz University, Shiraz, Iran*
[b] *Department of Materials Science and Engineering, Sharif University of Technology, Tehran, Iran*

ARTICLE INFO

ABSTRACT

In this study, electrolytic plasma processing (EPP) was employed for surface nitrocarburizing of AISI 1020 steel in a urea electrolyte, where the substrate samples were connected cathodically to a high-voltage DC current power supply. The structural, mechanical, wear and corrosion properties of the samples treated for 3–5 min were investigated. The results show that the surface layers formed on the samples by this treatment at 220 V have a ferritic nitrocarburizing characteristic which consists of a compound layer and diffusion zone. The surface layers of the treated samples at 240 V consisted of a compound layer, martensitic layer and diffusion zone, respectively, which is a marker of austenitic nitrocarburizing. The compound layers formed at 220 V and 240 V consisted of ε-Fe$_{2\text{-}3}$ (N,C) and γ'-Fe$_4$ (N,C) phases. The hardness value of the compound layer on the substrate was about 930 HV which was 4.5 times higher than that of the substrate. The thickness of the surface layer formed on the samples was a function of time and applied voltage. The wear and corrosion resistances of the samples were improved due to the surface treatment.

1. Introduction

Nitrocarburizing is a thermo-chemical process that consists of diffusing nitrogen and carbon into the surface of ferrous materials. The structural evolution produced by this treatment can be subdivided into a compound layer (often called white layer), consisting predominantly of iron carbonitrides (ε-Fe$_{2\text{-}3}$ (N,C)/or γ'-Fe$_4$ (N,C)) phases which is responsible for good tribological and anticorrosion properties of the surface, and a diffusion zone, where N and C are dissolved interstitially in the ferritic matrix, leading to the improvement of fatigue resistance. In comparison to other surface engineering technologies, nitrocarburizing is distinguished by its low treatment temperature and short treatment time, and high degree of shape and dimensional stability. Nitrocarburizing can be

applied in gas, liquid and plasma atmosphere. It is applied widely on various materials such as carbon steels, alloy steels, tool steels, stainless steels, cast iron and sintered materials [1–4]. The nitrocarburizing process, which is carried out at a temperature range of 550–580 °C, is called ferritic nitrocarburizing [5,6].

Although ferritic nitrocarburizing produces a compound layer with a high hardness and excellent tribological properties, the hardening response of the underneath nitrogen diffusion zone is relatively poor in plain carbon steels, and under high intensity loading conditions will fail prematurely due to its relatively low load bearing capacity. In order to solve this problem, attempts have been made to raise the nitrocarburizing temperature above Fe–N eutectoid point (∼590 °C) [5–7]. This process, which is termed austenitic nitrocarburizing, not only produces a hard surface layer and a diffusion zone, but also an iron–nitrogen–carbon austenite in the subsurface which is then transformed to martensite or bainite by quenching treatment [5–8].

The electrolytic plasma processing (EPP) technique was developed recently for the surface modification of steel in solution [9–13]. The electrolytic plasma process has a similar configuration to a conventional anodic oxidation or electroplating process. However, the applied electrode potential in all the electrolytic plasma processes is much higher than that of the conventional process. In this method under certain conditions, the electrode process rates are so high that the gaseous products of electrolysis do not have enough time to leave the surface of the metal electrode. So that, at a critical applied voltage, it is separated from the electrolyte by a so-called "vaporgaseous" envelope (i.e. a mixture of vaporized electrolyte and gases evolving from the electrode processes). The strong electric field in this envelope causes the ionization of the gaseous products and thus generates an electrical discharge at the electrode surface [9,10]. In the plasma discharge channel/area, plasma chemical interaction occurs and oxide or nitride can be formed on the substance surface to be treated [9,14,15].

In this study, electrolytic plasma nitrocarburizing (EPN/C), which is a cathodic process, was applied on AISI 1020 steel in an aqueous solution which consists of water, urea and sodium carbonate. Nie et al. [16] reported nitrocarburizing of AISI 1020 steel using EPP technique in a formamide based electrolyte which is toxic and flammable. There is also some published reports [17,18] on nitrocarburizing of stainless steel in electrolytes consisting of urea. However, to the best of our knowledge, nitrocarburizing of AISI 1020 plain carbon steel in electrolytes including urea has not been done. This electrolyte is a cost effective, environmentally friendly and non-hazardous compared to the previously employed organic electrolytes [16]. Our main purpose in this work is the nitrocarburizing of AISI 1020 steel by EPP in an electrolyte including urea and the investigation of the effect of applied voltage and time of the treatment on the structure, mechanical and corrosion properties of the treated specimens.

2. Experimental procedure

AISI 1020 steel disk specimens (25 mm in diameter and 5 mm in thickness) were used for the experiments. The specimens
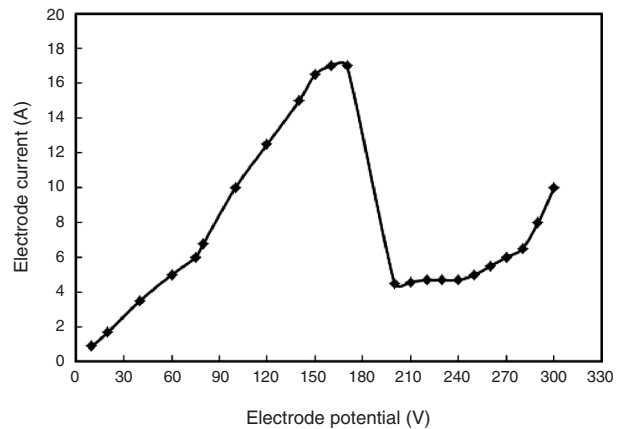

Fig. 1 – Current–voltage characteristic of the electrodes.

were normalized at 920 °C for 20 min, and then were air cooled. The specimens were polished to 1 μm using standard metallographic techniques. The specimens were connected to the negative terminal of a 40 kW DC power supply with a high current capability and were immersed in the bath to a depth of 30 mm beneath the electrolyte surface. The counter electrode (anode) was a stainless steel plate immersed in the electrolyte, and its area was significantly larger than that of the sample, so that the anode surface was 55 times larger than that of the cathode. The electrolyte was prepared from an aqueous solution of urea ($H_2N–CO–NH_2$) in distilled water, and sodium carbonate was added to electrolyte for the adjustment of electrical conductivity. In this research, the EPN/C process was performed via a rapid increase of the voltage in the initial stage (0–170 V). When the plasma envelope was established, the voltage was adjusted to 220 V or 240 V. The process was conducted for either 3 or 5 min at a current density of 0.5 A/cm². The current–voltage characteristic of the EPN/C treatment is illustrated in Fig. 1.

Fig. 2 shows the plasma environment around the cathode in the region of 200–270 V. The surface temperature of the specimens used in this work was measured with K-type thermocouple, and the temperature was estimated as 570 °C at 220 V and 715 °C at 240 V.

Fig. 3a and b shows the relationship of the electrode voltages, specimen surface temperature and current density. After the treatment, the phases of the compound layer were identified by a Philips X-ray diffractometer with Cu Kα radiation.

For microstructure characterizations, the samples were mounted, mechanically polished and etched in 2% Nital. Then, the layer structure and thickness of the compound layer were examined by Nikon optical microscopy and Oxford-5526 scanning electron microscope (SEM). The variation in hardness with depth was determined using a Leitz-Wetzlar microhardness tester under a load of 25 g. The case depth (thickness) of the diffusion zone is defined as the depth at which the hardness is at least 10% above the core hardness. Unlubricated wear studies were carried out using a pin-on-disc machine. The discs were run against stationary pins 3 mm in diameter and made of hardened SAE 52100 chrome bearing steel. A normal load of 60 N and a sliding speed of 0.1 m/s were employed. The tests were run for different sliding distances up to a
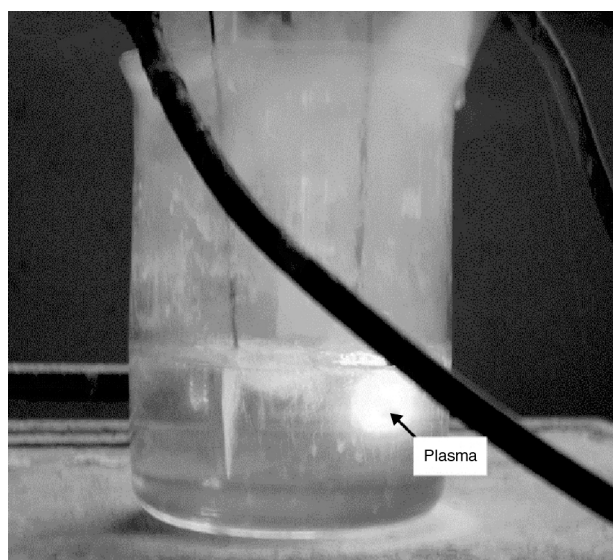
Fig. 2 – Plasma environment around the cathode or work piece.

maximum of 1 km and weight loss was measured in each case using a sensitive electronic balance with a measuring accuracy of 10^{-4} g.

Potentiodynamic polarization tests were carried out for the untreated and nitrocarburized samples at 25 °C using a Metrohm 628-10 potentiostat using a GPES software of the AutoLab system. A three-electrode cell with the untreated or nitrocarburized samples as the working electrode, Ag-AgCl

Fig. 3 – Relationship of the electrode voltages with (a) the specimen temperature and (b) the current density in the EPN/C treatment.

saturated electrode as the reference electrode and a platinum rod as the counter electrode were used in these tests. In order to obtain a steady-state condition before potentiodynamic polarization tests, the samples were immersed in the electrolyte for 24 h in the open circuit condition. Afterwards, the potentiodynamic polarization curves were obtained at a scan rate of 1 mV/s from −300 mV to +300 mV vs. open circuit potential (OCP). The test cell contained 3% NaCl solution (pH = 6.8). To get reliable results, the polarization experiments were repeated three times.

3. Results and discussion

3.1. Structural analysis

The effect of the voltage and time of the EPN/C treatment on the thickness of the compound layer and hardened subsurface layer is summarized in Table 1. The results show that the thickness of the compound layer (or white layer) and hardened subsurface layer is a function of the applied voltage (and thus temperature) and treatment time, and increases as the voltage and/or time increases.

Fig. 4 shows the cross-sectional optical micrographs of the EPN/C specimens. The influence of the applied voltage and time of the treatment on the white layer growth can be seen in the micrographs. In Fig. 4c and d corresponding, to samples 3 and 4, a zone between the white and diffusion layers, which is a mixture of martensite and retained austenite, can be observed. This structure is related to the austenitic nitrocarburizing treatment. Nevertheless, as shown in Fig. 4a and b corresponding to samples 1 and 2, the surface hardened layers only consisted of the white layer and diffusion layer which have the structural characteristic of ferritic nitrocarburizing. In the EPN/C treatment, the samples have no contact with the electrolytic environment during nitrocarburizing; however, at the end of the treatment and after turning off the electrode current, contact is made between the samples and electrolyte, and the samples are quenched in the electrolyte environment. Therefore, the electrolytic media is both heat-treating and quenching environments.

For samples 3 and 4, since the treatment temperature is higher than the eutectoid temperature of Fe–N, an iron–nitrogen–carbon austenite will be created in the subsurface, as reported by Bell et al. [5]. The subsurface will be changed to a mixture of martensite and retained austenite during the direct quench after turning off the electrical current because the samples are quenched in the electrolytic environment. The austenite layer, formed beneath the white layer, is stabilized by dissolved nitrogen. This layer would reach the maximum hardness or strength of the subsurface by a phase transformation from austenite to martensite which can be obtained by quenching from the treatment temperature. Though, direct quenching cannot form a fully martensitic structure in the sublayer [5]. Therefore, some retained austenite still exists in the austenite sublayer (Fig. 4c and d), since nitrogen which is a powerful austenite stabilizer depresses M_f (martensite finish temperature) below room temperature [8].
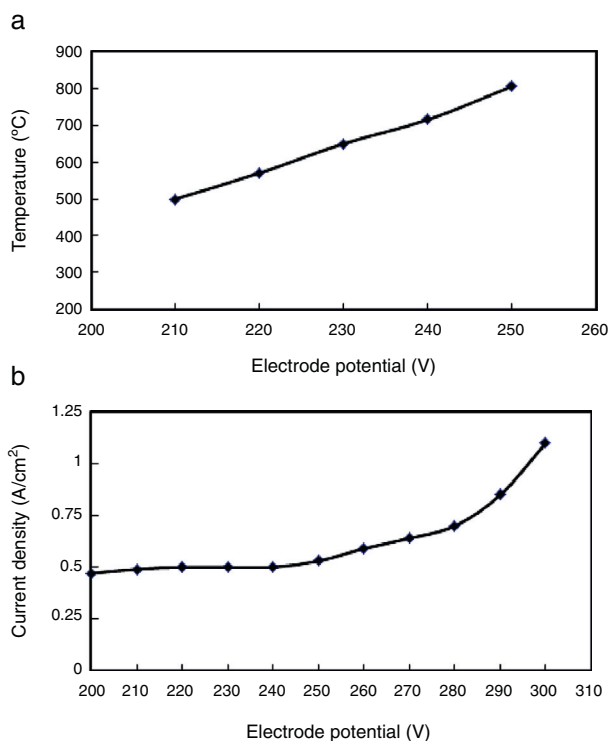
Table 1 – Effect of the voltage and time of the EPN/C treatment on the treated samples.

| Sample no.	Structural properties		Treatment parameters		
	Compound layer thickness (μm)	Hardened subsurface layer thickness (μm)	Voltage (V)	Time (min)	Temperature (°C)
1	16–17	50–55	220	3	570
2	24–26	100–101	220	5	570
3	21–22	120–135	240	3	715
4	28–29	180–200	240	5	715

3.2.   SEM investigation

Fig. 5a and b shows the SEM images of samples 2 and 4. The SEM studies revealed that a uniform and compact white layer was firmly developed on the surface of the steel, and no crack was observed between the white layer and substrate. The compound layer formed during nitrocarburizing treatment includes poly phase iron nitrides or iron carbonitrides such as γ'-Fe_4N or γ'-Fe_4 (N,C) and ε-$Fe_{2-3}N$ or ε-Fe_{2-3} (N,C) [4,19]. It is difficult to determine whether the phases on the compound layer are nitride or carbonitrides, as the lattice spacing in iron nitride or carbonitrides are nearly the same [4,19]. However, it may be assumed that γ' and ε phases are carbonitride, since the gas mixture around cathode or workpiece contains CO_2. In highly conductive solutions of urea, the cathodic process of hydrogen formation is also accompanied with a reduction of ammonia [17,20], which can be expressed by the net reaction:

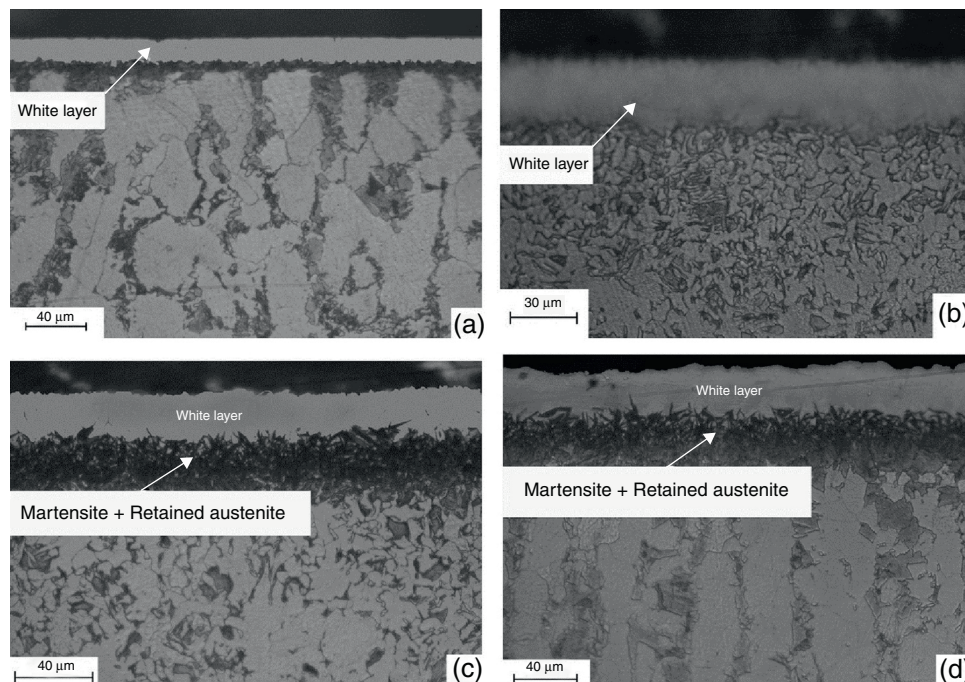$$3(NH_2)_2CO + 9H_2O + 6e^- \rightarrow 6NH_3\uparrow + 3CO_2\uparrow + 3H_2\uparrow + 6OH^- \tag{1}$$
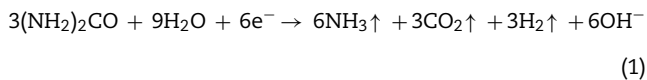
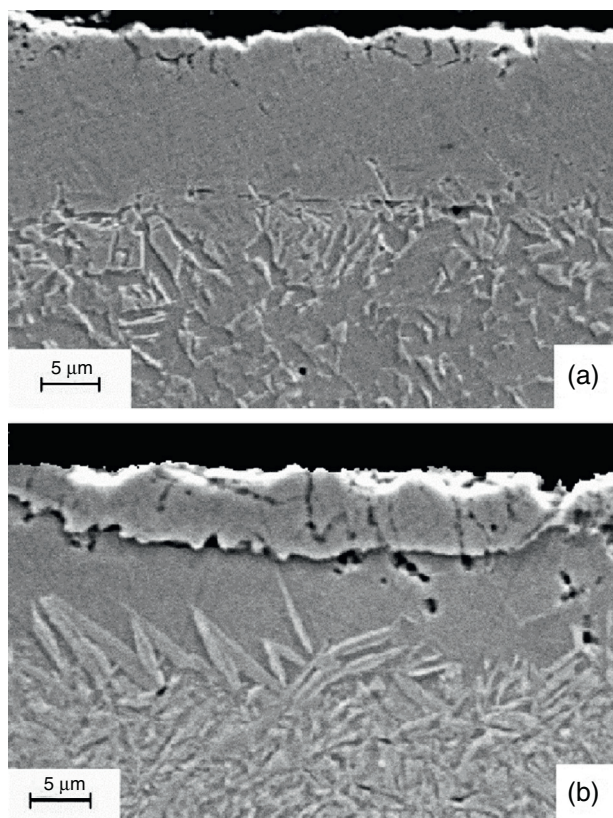The above reaction is predominated at low voltages (below 75 V), whereas above 75 V a significant amount of additional gas (i.e. vaporized electrolyte) is also produced near the sample surface due to ohmic heating of the local electrolyte solution [9,17]:

$$(NH_2)_2CO \cdot nH_2O \xrightarrow{T)T_v} 2NH_3\uparrow + CO_2\uparrow + (n-1)H_2O\uparrow \tag{2}$$
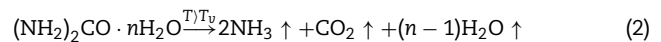
where T_v is the vaporization temperature of the electrolyte solution. The evaporation-decomposition in Eq. (2) depends on the current density which obviously is higher on the smaller (i.e. cathode in our case) electrode. Therefore, within the voltage range of 75–150 V, the gaseous products from the reactions in Eqs. (1) and (2) evolve rapidly and form a vapor envelope which separates the sample surface from the electrolyte. This low conductive envelope is subsequently electrically broken down at a certain voltage (∼170 V). At this voltage, the electric field strength within this region reaches a value between 10^6 V/m and 10^8 V/m [9] which is sufficient for the initiation of ionization process in the vapor envelope. The ionization phenomenon appears initially as a rapid sparking in scattered gaseous bubbles and then is transformed into a uniform glow distributed throughout the vapor plasma envelope. The complete separation of the sample from the electrolyte by the vapor/plasma envelope in the region (200–270 V) causes a

Fig. 4 – Optical micrographs of the cross section of the EPN/C treated samples (a) sample 1, (b) sample 2, (c) sample 3, and (d) sample 4.

Fig. 6 – XRD pattern of the EPN/C treated samples.

detected. γ' phases are indicators of nitrocarburized layer and these changes were outcomes of phase transformation in the white layer.

Besides, ε-Fe$_{2-3}$ (N,C) phases are indicators for white layer. XRD results of all samples show the peaks of ε (1 0 0) and ε (1 0 1); increasing the thickness of nitrocarburized layers amplifies the peak intensities of these phases.

3.4.   Mechanical properties

The Vickers microhardness measurements were made on the metallographic specimens and the profiles are shown in Fig. 7a and b. The hardness value of the compound layer was about 930 HV, whereas the hardness value of the substrate was 205 HV. The profiles visibly indicate that the hardness decreases from the nitrocarburized layer to the substrate. The change in hardness beneath the compound layer in samples 3 and 4 shows a smoother decrease compared with samples 1 and 2, which is due to the presence of a martensitic layer between the compound layer and the diffusion layer, and also the higher thickness of the diffusion layer in these samples.

3.5.   Tribological properties

To evaluate the wear properties of the treated samples, the wear tests were performed on a dry pin-on-disc tester. The weight loss vs. sliding distance relationship is shown in Fig. 8a and b. The results show that the wear properties of the treated specimens have largely increased, since the ε and γ' iron carbonitrides have been formed on the surface, and the wear properties of samples 3 and 4 are relatively better than those of samples 1 and 2. This is attributed to the presence of ε carbonitride as the main phase in the surface layer of samples 3 and 4.

In order to analyze the tribological behavior of the specimens, the wear tracks on the specimen surfaces were investigated. There are two major categories of wear mechanisms: adhesive and abrasive wear. Adhesive wear occurs when the contact pressure between the rolling surfaces is high enough to cause local plastic deformation and welding

Fig. 5 – SEM micrographs of the cross section of the EPN/C treated samples (a) sample 2 and (b) sample 4.

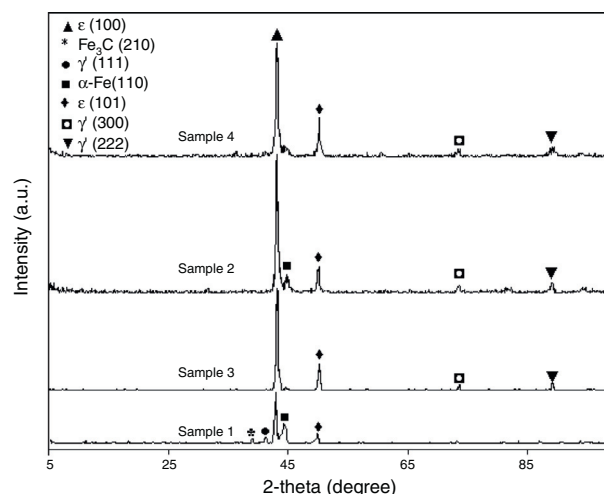sharp reduction in the electrode current from approximately 17 A to 4 A (Fig. 1).

Beyond 270 V, the glow discharge is transformed into intensive arcing accompanied by a low frequency acoustic emission. The plasma generated in the vapor-gaseous envelope in the region of 200–270 V produces a high concentration of nitrogen and carbon-containing radicals and ionic components. Under the action of both the applied voltage and hydrodynamic forces, these components bombard the sample surface and make a high rate of diffusional flow toward the growing surface layer [9,10,17].

3.3.   XRD analysis

The XRD results of the electrolytic plasma nitrocarburized specimens as a function of the process voltage are shown in Fig. 6. The XRD analysis of sample 1 shows the peaks of ε-Fe$_{2-3}$ (N,C) with some γ'-Fe$_4$ (N,C), α-Fe and Fe$_3$C phases. For other samples with a thicker white layer the peak of Fe$_3$C (2 1 0) disappeared. This could be explained by the white layer thickness; X-ray could not reach to and/or reflect from the crystal structure of the matrix when the white layer was thick enough.

As can be seen in Fig. 4, in samples 3 and 4, there is a martensitic layer beneath the white layer which make them differ from samples 1 and 2. Because of this martesitic layer, XRD results could not reveal the α-Fe phase of the matrix.

Moreover, for samples 2, 3, and 4, XRD patterns showed that γ' (1 1 1) phase disappeared and γ' (3 0 0) and γ' (2 2 2) phases

Table 2 – Corrosion current densities and corrosion potential voltages of untreated and treated samples.					
Sample no.	Untreated	1	2	3	4
V_{Corr} (V)	−0.795 ± 0.004	−0.592 ± 0.002	−0.575 ± 0.003	−0.562 ± 0.002	−0.545 ± 0.003
i_{corr} (μA/cm^2)	12.21 ± 0.04	10.12 ± 0.04	9.92 ± 0.02	9.61 ± 0.03	9.45 ± 0.01

between the contacting asperities. Abrasive wear occurs when hard debris particles are indented and make a groove in the rolling surface of the material [4].
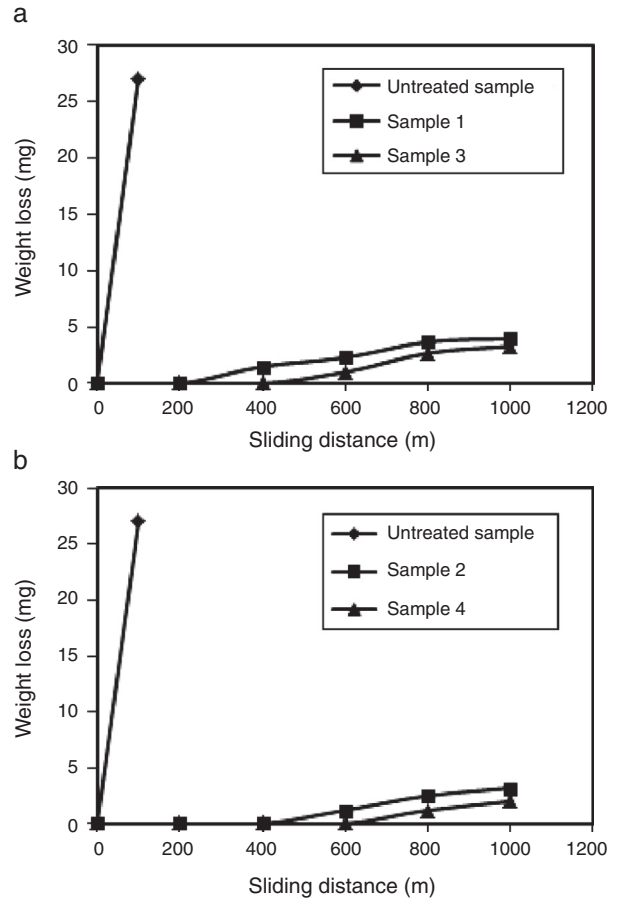
Fig. 9 shows the wear scars of the worn surfaces after 100 m and 1000 m sliding distance for the untreated and EPN/C treated samples, respectively. The untreated sample in Fig. 9a shows adhesive wear on the surface, and the wear tracks of this sample have been formed by microploughed and squeezed plastic deformation. Whereas sample 4 (Fig. 9b) showed even abrasive wear tracks and the much less failure was observed compared to the untreated sample. The similar abrasive wear tracks were observed for the other EPN/C treated samples.

3.6. Corrosion studies

The potentiodynamic polarization curves for the treated and untreated samples are shown in Fig. 10. The corrosion current densities and corrosion potential voltages of untreated and treated samples are presented in Table 2, as determined based on the classic Tafel analysis by extrapolating the

Fig. 8 – Wear plots of the EPN/C treated and untreated samples (a) samples 1 and 3 and (b) samples 2 and 4.

linear portions of the potential vs. log current plot back to their intersection.

The corrosion potential of nitrocarburized samples increased from −795 mV (for the untreated substrate) to noble potential. Also, the corrosion current densities for treated samples were lower than that for the untreated sample. The samples treated at 240 V show slightly better corrosion properties compared to the samples treated at 220 V. This effect was because of the higher thickness of nitrocarburized layer in samples 3 and 4.

Although the corrosion resistance of the samples nitrocarburized at 220 V and 240 V has been improved in comparison with the untreated sample, as reported by Lee et al. [21], to increase the corrosion resistance of nitrocarburized AISI 1020 steel, post oxidation treatment must be done on it. An adherent Fe_3O_4 oxide film with 0.2–1 μm thick on the compound layer, as the post-oxidizing of the nitrocarburized steels, enhances the corrosion resistance [5,21].

Fig. 7 – Microhardness profiles of the EPN/C treated samples (a) samples 1 and 3 and (b) samples 2 and 4.
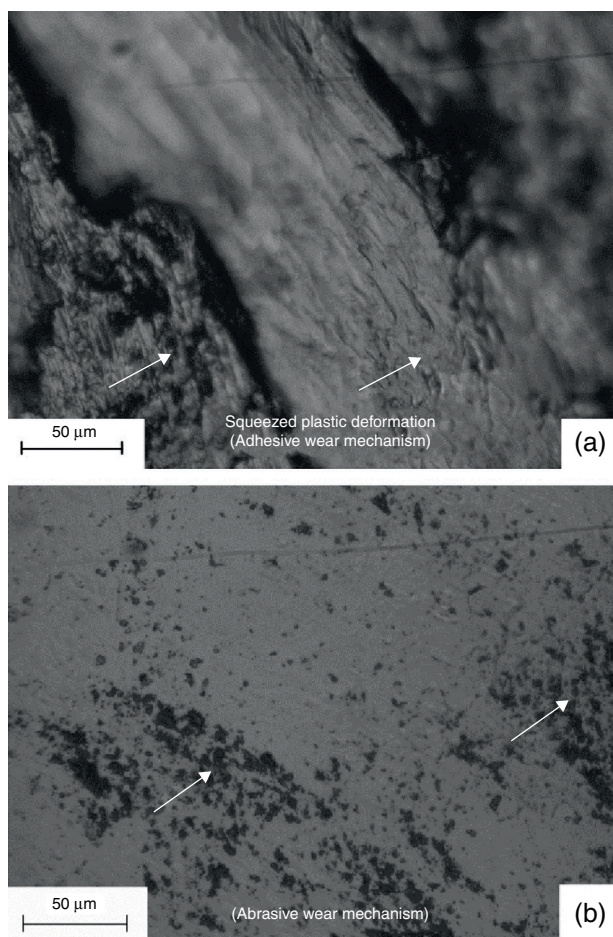
Fig. 9 – Optical micrographs of the wear tracks produced after (a) 100 m sliding distance for the untreated sample and (b) 1000 m sliding distance for sample 4.
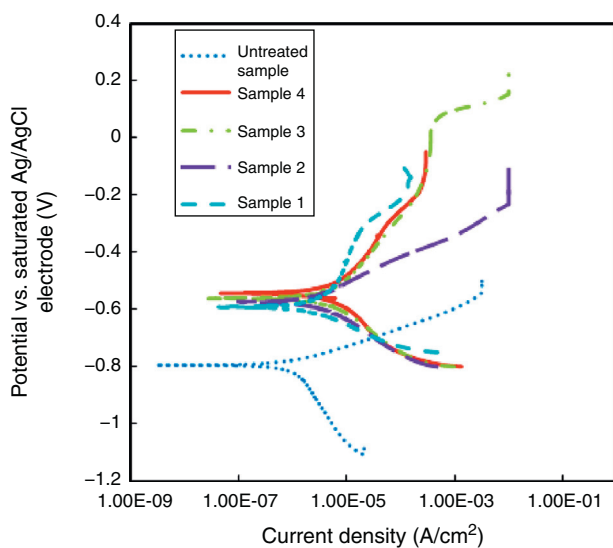
Fig. 10 – Potentiodynamic polarization curves for the EPN/C treated samples and the untreated sample.

4.   Conclusions

The AISI 1020 plain carbon steel was nitrocarburized in an urea aqueous solution by the EPP technique at 220 V and 240 V successfully. The following conclusions can be drawn from the present study:

- The surface layer formed on the samples by this treatment at 220 V has a characteristic of ferritic nitrocarburizing, i.e. the produced surface layer at this voltage consists of the compound layer and diffusion zone. The surface layers of the treated samples at 240 V consisted of compound layer, martensitic layer and diffusion zone respectively, i.e. the austenitic nitrocarburizing treatment.
- The compound layer formed on the surface of the samples predominantly was consisted of ε-iron carbonitride. Some γ'-iron carbonitride, α-Fe and Fe_3C were also observed in samples treated at 220 V, while α-Fe and Fe_3C phases were disappeared by increasing the voltage to 240 V because of a martensitic layer beneath the white layer.
- For all thicknesses of the compound layers, ε-iron carbonitride are identifiable. Also, γ'-iron carbonitride would be detected in XRD spectra. However, changing time and temperature results in some phase transformations of this phase.
- The thickness of the compound layer and hardened subsurface layer is very sensitive to the time and final voltage and increases as the time and voltage increase.
- The change in hardness beneath the compound layer in the samples treated at the voltage of 240 V shows smoother decrease compared to the samples treated at voltage of 220 V, which is due to the presence of a martensitic layer between the compound layer and diffusion layer, and also the higher thickness of the diffusion layer in these samples.
- The wear properties of the nitrocarburized samples were increased significantly in relation to the untreated sample. The samples treated in 240 V, due to the formation of martensite subsurface layer and single ε phase on the surface, presented better wear properties than those treated in 220 V.
- The corrosion resistance of the nitrocarburized samples was increased in relation to the untreated sample. Besides, the samples treated at 240 V showed somewhat better corrosion properties compared to the samples treated at 220 V.

Conflicts of interest

The authors declare no conflicts of interest.

Acknowledgements

REFERENCES

[1] Qiang YH, Ge SR, Xue QJ. Sliding wear behavior of nitrocarburized bearing steel. Mater Sci Eng A 2000;278:261–6.

[2] Pereloma EV, Conn AW, Reynoldson RW. Comparison of ferritic nitrocarburizing technologies. Surf Coat Technol 2001;145:44–50.

[3] Teimouri M, Ahmadi M, Pirayesh N, Aliofkhazraei M, Mousavi Khoee M, Khorsand H, et al. Study of corrosion behavior for nitrocarburized sintered Astaloy CrM®+C. J Alloys Compd 2009;477:591–5.

[4] Karakan M, Alsaran A, Celik A. Effect of process time on structural and tribological properties of ferritic nitrocarburizing AISI 4140 steel. Mater Design 2004;25:349–53.

[5] Bell T, Sun Y, Suhadi A. Environmental and technical aspects of plasma nitrocarburizing. Vacuum 2000;59:14–23.

[6] Bell T. Gaseous and plasma nitrocarburizing. ASM Handbook 1998;4:425–35. ASM.

[7] Fattah M, Mahboubi F. Comparison of ferritic and austenitic plasma nitriding and nitrocarburizing behavior of AISI 4140 low alloy steel. Mater Design 2010;31:3915–21.

[8] Krishnaraj N, Iyer K, Sundaresan S, Srinivasan PB. Optimization of compound layer thickness for wear resistance of nitrocarburized H11 steel. Wear 1998;215:123–30.

[9] Yerokhin AL, Matthews A, Nie X, Leyland A. Plasma electrolysis for surface engineering. Surf Coat Technol 1999;122:73–93.

[10] Gupta P, Tenhundfeld G, Daigle EO, Ryabkov D. Electrolytic plasma technology: science and engineering—an overview. Surf Coat Technol 2007;201:8746–60.

[11] Bejar MA, Henriquez R. Surface hardening of steel by plasma-electrolysis boronizing. Mater Design 2009;30:1726–8.

[12] Bayati MR, Molaei R, Janghorban K. Surface modification of AISI 1045 carbon steel by the electrolytic plasma process. Metall Mater Trans A 2010;41A:906–11.

[13] Çavuşlu F, Usta M. Kinetics and mechanical study of plasma electrolytic carburizing for pure iron. Appl Surf Sci 2011;457:4014–20.

[14] Lv G, Gu W, Chen H, Feng W, Latif Khosa M, Li L, et al. Characteristic of ceramic coatings on aluminum by plasma electrolytic oxidation in silicate and phosphate electrolyte. Appl Surf Sci 2006;253:2947–52.

[15] Shokouhfar M, Dehghanian C, Baradaran A. Preparation of ceramic coating on Ti substrate by plasma electrolytic oxidation in different electrolytes and evaluation of its corrosion resistance. Appl Surf Sci 2011;257:2617–24.

[16] Nie X, Hao Q, Wei M. A novel modification technique for metal surface. J Wuhan Univ Technol 1996;11:28–35.

[17] Nie X, Tsotsos C, Wilson A, Yerokhin AL, Leyland A, Matthews A. Characteristics of a plasma electrolytic nitrocarburizing treatment for stainless steels. Surf Coat Technol 2001;139:135–42.

[18] Tsotsos C, Yerokhin AL, Wilson AD, Leyland A, Matthews A. Tribological evaluation of AISI 304 stainless steel dublex treated by plasma electrolytic nitrocarburising and diamond-like carbon coating. Wear 2002;253:986–93.

[19] Maliska AM, Oliveria AM, Klein AN, Muzart JLR. Surface porosity sealing effect of plasma nitrocarburizing on sintered unalloyed iron. Surf Coat Technol 2001;141:128–34.

[20] Osetrova NV, Skundin AM. Anodic oxidation of urea in neutral solutions. Russ J Electrochem 1994;30:1145–7.

[21] Lee KH, Nam KS, Shin PW, Lee DY, Song YS. Effect of post-oxidizing time on corrosion properties of plasma nitrocarburized AISI 1020 steel. Mater Lett 2003;57:2060–206.